

## Generation and control of population difference gratings in a three-level hydrogen atomic medium using half-cycle attosecond pulses nonoverlapping in the medium

Rostislav Arkhipov<sup>1,2</sup>, Mikhail Arkhipov<sup>1,2</sup>, Anton Pakhomov<sup>1</sup>, Olga Diachkova<sup>1,2</sup> and Nikolay Rosanov<sup>1,2</sup>

<sup>1</sup>*St. Petersburg State University, Faculty of Physics, Universitetskaya Náberezhnaya 7/9, St. Petersburg 199034, Russia*

<sup>2</sup>*Ioffe Institute, Politekhnicheskaya Street 26, St. Petersburg 194021, Russia*



(Received 20 February 2024; accepted 23 May 2024; published 11 June 2024)

Recently, the possibility of the generation and interaction of unipolar half-cycle electromagnetic pulses with quantum systems has been the subject of active research. Such pulses can find many different and interesting applications. They are able to excite quantum systems very fast. Based on the numerical solution of Maxwell-Bloch equations, this paper studies theoretically the possibility of guiding and ultrafast controlling population difference gratings by a sequence of half-cycle attosecond pulses in a three-level resonant medium. The parameters of the model medium (transition frequencies and transition dipole moments) match those in a hydrogen atom. We show the possibility of guiding periodic gratings and dynamic microcavities on different resonant transitions in the medium. We also consider the superradiance of polarization waves and atomic gratings produced by half-cycle pulses.

DOI: [10.1103/PhysRevA.109.063113](https://doi.org/10.1103/PhysRevA.109.063113)

### I. INTRODUCTION

The study of the generation and interaction of ultrashort electromagnetic pulses with matter has been one of the most important topics in modern optics since the advent of the first lasers [1]. Attosecond pulses are now in active use for ultrafast control of electron dynamics in matter [2–6]. Progress in this field has led to the award of the Nobel Prize in Physics in 2023. This underlines the importance and relevance of this direction in modern physics [7].

The pulses obtained in these studies consist of multiple half waves, i.e., they are bipolar. If all but one of the half waves are cut off, we obtain pulses of shortest duration in a given spectral range, the so-called unipolar half-cycle pulses [8,9]. For pulses of this type, an important characteristic is the electric pulse area. It is defined as the integral of the electric-field strength  $\vec{E}$  over time  $t$  at a given point in space  $\vec{r}$  [10–12]:

$$\vec{S}_E(\vec{r}) = \int_{-\infty}^{+\infty} \vec{E}(\vec{r}, t) dt. \quad (1)$$

In practice, it is difficult to obtain strictly unipolar pulses. However, in some cases it is possible to obtain pulses with a shape close to unipolar pulses, which have a pronounced half-wave field and trailing edge of the opposite polarity [2,8,13–25]. Purely unipolar pulses are also possible in some cases [9,23,26–28]. Provided this trailing edge is weak and long, it has no effect on the quantum system. Subcycle pulses can affect it, as it is purely unipolar [29–31]. Therefore, in the following we consider the effect of a pure unipolar half-cycle pulse without a trailing edge. This can be a good approximation to the experimental half-cycle pulses.

Such pulses have attracted the attention of researchers because of the peculiarities of their effect on micro-objects: They can be rapidly excited by transmitting a mechanical

momentum to a charged particle in one direction [8,32–34]. This opens up the possibility of using them in a variety of applications, e.g., ultrafast control of atoms, molecules, and nanostructures [29,32–36] and holography with ultrahigh resolution of fast-moving objects [37] (see [8] for an overview of recent research in this direction).

The possibility of generating population difference gratings in a resonant medium is one such interesting application. In general, the interference of two or more coherent quasi-monochromatic laser beams is used to create such gratings when the beams are superimposed in the medium [38]. The gratings produced in this way find various applications in optics. For example, they are used as Bragg mirrors in optical fibers [39,40]. However, the possibility of ultrafast control of such gratings, i.e., turning them on, turning them off, changing their period, etc., is obviously hampered by the traditional way of creating gratings based on the interference of overlapping monochromatic beams. Ultrashort [41–43] and extremely short pulses (ESPs) are very well suited for this purpose [44–48]. Previously, the first experiments in which a photon echo was formed demonstrated the formation of gratings by nanosecond laser pulses that do not overlap in the medium [41,42]. The gratings that were created in this case have found application in echo holography [49,50]. However, ultrafast control of such gratings is not possible with long multicycle pulses.

In a given spectral interval, half-cycle pulses have the shortest duration [8]. In the case of half-cycle pulses, direct interference in the conventional sense is impossible. However, in this case it is possible to generate population gratings due to the interference of the electric areas of the pulses [51]. On closer examination, the formation of the gratings can be explained by the interference of the polarization waves induced by the previous pulse with those of the following pulse [44,45]. The possibility of studying and controlling

gratings with single- and half-cycle pulses has been studied previously in various approximations (a two-level medium, small-field-amplitude approximation in a rarefied medium without consideration of propagation effects, sudden perturbation approximation, etc.) [44–48]. See [52] for a review of the results of early studies. Such approaches are very simplistic as they do not take into account the spatiotemporal dynamics of the polarization and the inversion in a multilevel medium, which are to exhibit much more complex dynamics.

Sometimes the question of grating formation in a real multilevel medium by ESPs makes researchers skeptical. This casts doubt on some studies of how subcycle pulses interact with matter in the two-level approximation. Furthermore, the coherent propagation of subcycle pulses in matter has mainly been the subject of two-level approximation studies [53–59]. Including additional levels can lead to the complex behavior of coherent phenomena, such as photon echo [60]. This raises the urgent question of conducting these studies using more realistic multilevel models, considering spatial and temporal dynamics of the field, medium polarization, and population of levels.

We also note that in our case the refractive index of the medium changes rapidly in both space and time. Our medium is therefore an example of a spatiotemporal photonic crystal (STPC) [61–63]. Such media have been a very interesting subject of research in recent times (see the reviews in [64–67]). In addition to their fundamental importance, they are also of interest for their potential use in frequency conversion of reflected radiation [66], creation of novel laser sources [65,68], and other uses [67]. Therefore, the issues discussed below may be interesting from the viewpoint of creating and controlling STPC properties.

The aim of this paper is to analyze theoretically the possibility of generating and controlling gratings using a sequence of half-cycle attosecond pulses in an extended three-level medium. The theoretical analysis is based on the numerical solution of the material equations for a three-level medium coupled to the wave equation. In this analysis, the pulses did not overlap in the medium. Atomic hydrogen was used as the resonant medium.

In contrast to previous studies of two- [44,45] and three-level rubidium atomic media [69], which primarily yielded harmonic gratings, here we present a more complex and unusual dynamics of the structures. The shape of the population grating not only differs from a harmonic one, but also varies at different resonant transitions in the medium. This work is an extension of previous studies in the two-level and other aforementioned approximations that aims at broadening its scope. The superradiance of the induced polarization waves and gratings is also considered.

## II. THEORETICAL MODEL AND SYSTEM UNDER CONSIDERATION

The effects of the propagation of ESPs in an extended medium must be taken into account for a more accurate study. In this case, a joint numerical solution of the system for the density matrix of a three-level medium and the wave

equation for the electric field was performed. This system of equations has the form [70,71]

$$\begin{aligned} \frac{\partial}{\partial t} \rho_{21} = & -\frac{\rho_{21}}{T_{21}} - i\omega_{12}\rho_{21} - i\frac{d_{12}E}{\hbar}(\rho_{22} - \rho_{11}) \\ & - i\frac{d_{13}E}{\hbar}\rho_{23} + i\frac{d_{23}E}{\hbar}\rho_{31}, \end{aligned} \quad (2)$$

$$\begin{aligned} \frac{\partial}{\partial t} \rho_{32} = & -\frac{\rho_{32}}{T_{32}} - i\omega_{23}\rho_{32} - i\frac{d_{23}E}{\hbar}(\rho_{33} - \rho_{22}) \\ & - i\frac{d_{12}E}{\hbar}\rho_{31} + i\frac{d_{13}E}{\hbar}\rho_{21}, \end{aligned} \quad (3)$$

$$\begin{aligned} \frac{\partial}{\partial t} \rho_{31} = & -\frac{\rho_{31}}{T_{31}} - i\omega_{13}\rho_{31} - i\frac{d_{13}E}{\hbar}(\rho_{33} - \rho_{11}) \\ & - i\frac{d_{12}E}{\hbar}\rho_{32} + i\frac{d_{23}E}{\hbar}\rho_{21}, \end{aligned} \quad (4)$$

$$\begin{aligned} \frac{\partial}{\partial t} \rho_{11} = & \frac{\rho_{22} + \rho_{33}}{T_{11}} + i\frac{d_{12}E}{\hbar}(\rho_{21} - \rho_{21}^*) \\ & - i\frac{d_{13}E}{\hbar}(\rho_{13} - \rho_{13}^*), \end{aligned} \quad (5)$$

$$\begin{aligned} \frac{\partial}{\partial t} \rho_{22} = & -\frac{\rho_{22}}{T_{22}} - i\frac{d_{12}E}{\hbar}(\rho_{21} - \rho_{21}^*) \\ & - i\frac{d_{23}E}{\hbar}(\rho_{23} - \rho_{23}^*), \end{aligned} \quad (6)$$

$$\begin{aligned} \frac{\partial}{\partial t} \rho_{33} = & -\frac{\rho_{33}}{T_{33}} + i\frac{d_{13}E}{\hbar}(\rho_{13} - \rho_{13}^*) \\ & + i\frac{d_{23}E}{\hbar}(\rho_{23} - \rho_{23}^*), \end{aligned} \quad (7)$$

$$P(z, t) = 2N_0 d_{12} \text{Re} \rho_{12} + 2N_0 d_{13} \text{Re} \rho_{13} + 2N_0 d_{23} \text{Re} \rho_{32}, \quad (8)$$

$$\frac{\partial^2 E(z, t)}{\partial z^2} - \frac{1}{c^2} \frac{\partial^2 E(z, t)}{\partial t^2} = \frac{4\pi}{c^2} \frac{\partial^2 P(z, t)}{\partial t^2}. \quad (9)$$

Here  $\rho_{11}$ ,  $\rho_{22}$ , and  $\rho_{33}$  are the populations of the first, second, and third states of the atom respectively;  $\rho_{21}$ ,  $\rho_{32}$ , and  $\rho_{31}$  are the nondiagonal elements of the density matrix determining the dynamics of the polarization of the medium;  $\omega_{12}$ ,  $\omega_{23}$ , and  $\omega_{13}$  are the transition frequencies of the medium;  $d_{12}$ ,  $d_{13}$ , and  $d_{23}$  are the dipole moments of these transitions; and  $\hbar$  is the reduced Planck constant. The equations also include relaxation terms  $T_{ik}$ .

The medium parameters (transition frequencies and transition dipole moments) have been chosen to be close to those for a hydrogen atom [72,73] (see Table I).

As initial conditions, a pair of half-cycle Gaussian pulses was sent from the boundaries of the integration region into the medium:

$$E(z = 0, t) = E_{01} e^{-(t-\Delta_1)^2/\tau^2}, \quad (10)$$

$$E(z = L, t) = E_{02} e^{-(t-\Delta_2)^2/\tau^2}. \quad (11)$$

Delays  $\Delta_1 = 2.5\tau$  and  $\Delta_2 = 29\tau$  were chosen in such a way that the pulses did not overlap simultaneously in the medium. The system of equations (2)–(9) has been solved numerically. The density-matrix equations (2)–(7) were solved by the fourth-order Runge-Kutta method. The solution of the wave equation (9) was done by the finite-difference time-domain

TABLE I. Parameters of the model and excitation pulses used in calculations.

Parameter	Value
transition frequency 12 (corresponding wavelength)	$\omega_{12} = 1.55 \times 10^{16}$ rad/s ( $\lambda_{12} = 121.6$ nm)
dipole moment of transition 12	$d_{12} = 3.27$ D
transition frequency 13 (corresponding wavelength)	$\omega_{13} = 1.84 \times 10^{16}$ rad/s ( $\lambda_{13} = 102.6$ nm)
dipole moment of the transition 13	$d_{13} = 1.31$ D
transition frequency 23 (corresponding wavelength)	$\omega_{23} = 2.87 \times 10^{15}$ rad/s ( $\lambda_{23} = 656.6$ nm)
dipole moment of transition 23	$d_{23} = 12.6$ D
atomic concentration	$N_0 = 10^{14}$ cm <sup>-3</sup>
pulse amplitude	$E_{01} = E_{02} = 45 \times 10^7$ V/cm
pulse duration	$\tau = 100$ as
relaxation times $T_{ik}$	$T_{ik} = 1$ ns

method. Three-dimensional propagation of half-cycle pulses can be described by the one-dimensional wave equation, for example, in coaxial waveguides, since they have no cutoff frequency [74].

The total length of the computational domain is  $L = 12\lambda_0$ . The medium was placed between the points  $z_1 = 4\lambda_0$  and  $8\lambda_0$ . In the calculations, as the pulses reached the boundaries of the integration domain, they were reflected from it and returned to the medium, but did not overlap. In Fig. 2, the movement of the pulses is shown schematically by arrows, where the digits denote the pulse number.

The three-level approximation serves as a convenient model of a resonant medium, as it already allows one to predict phenomena arising beyond the simplest two-level model [75]. In this sense the three-level model can be reasonably considered as a useful approach to study the few-cycle and subcycle pulse interaction with different resonant media. Regarding the contribution of ionization, as it was shown in [34], the ionization probability in these conditions (the pulse duration much less than the periods of medium transitions) is fully determined by the electric pulse area  $S_E$  or, to be more specific, by the ratio of the electric area of exciting pulses  $S_E$  to the certain atomic scale  $S_{at} = \hbar/ea_0$ , with the electron charge  $e$  and the radius of the first Bohr orbit  $a_0$ . The ionization becomes relevant when the electric area of exciting pulses  $S_E$  is comparable to  $S_{at}$  and can be neglected when  $S_E \ll S_{at}$ .

For the parameters given in Table I, we have  $S_E \approx 0.6S_{at}$ , so we can consider that the effect of the ionization is not so strong. If we reduce the amplitude of the electric field in the calculations to  $E_0 = 30 \times 10^7$  V/cm, the ratio  $S_E/S_{at} = 0.4$  is obtained. The amplitude of the gratings will decrease slightly in this case. However, in general, their spatiotemporal dynamics will remain qualitatively similar to those obtained with the parameters given in Table I.

It is worth emphasizing that the ionization phenomena would not cause the observed effects to disappear. Indeed, even for noticeable ionization probability, the excitation pulses would still cause population of excited levels and thus the waves of the induced medium polarization, so the population gratings would arise anyway due to the interference of these polarization waves with the consequent excitation pulses. However, ionization can indeed effect the parameters of these arising gratings, such as the modulation depth.

Furthermore, the results of the numerical solution of the time-dependent Schrödinger equation show that for half-cycle pulses shorter than the resonant transition periods, the probability of excitation and ionization of the quantum system also depends on the delay between pulses [31,76]. The second pulse can partially return the wave packet to the quantum well ionized by the first pulse, reducing the ionization probability.

It should be noted that some other recent studies have shown that coherent two-level dynamics can even survive for several Rabi cycles in the attosecond timescale, when the ionization is taken into account. Specifically, in Ref. [77] the authors report on the record fast attosecond Rabi oscillations in He atoms, where the resonant coupling of two-level bound-bound transitions prevails, in contrast with the dominance of bound-continuum transitions in the conventional strong-field infrared regimes. These findings also confirm the possibility of few-level models to describe the actual dynamics of multilevel media excited by strong and very short (attosecond) pulses. In addition, the carrier-wave Rabi flopping was observed in atomic [78] and semiconductor media [79] driven by few-cycle pulses.

### III. GRATING DYNAMICS WITH HALF-CYCLE PULSE EXCITATION

The results of the numerical integration of the system of equations (2)–(9) with the parameters given in Table I are shown in Figs. 1–4. Figure 1 illustrates the spatial and tem-

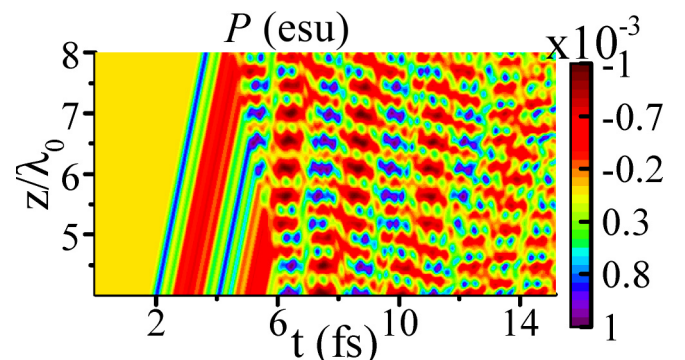


FIG. 1. Spatial and temporal dynamics of medium polarization  $P(z, t)$ .

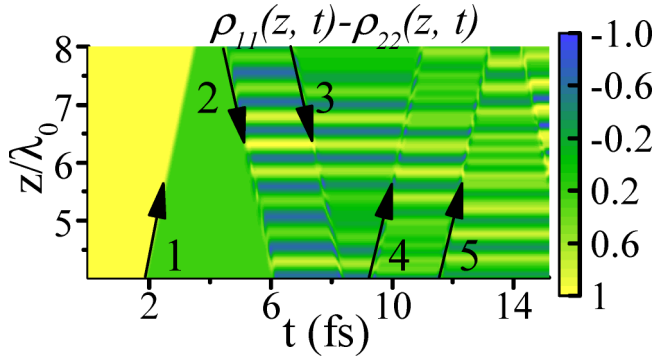


FIG. 2. Spatial and temporal dynamics of the medium population difference  $\rho_{11} - \rho_{22}$  under the action of half-cycle Gaussian pulses, with the directions of their propagation shown by arrows.

poral dynamics of the medium polarization  $P(z, t)$ . Figures 2 and 3 provide the population differences at the 1-2 and 2-3 transitions. Figure 4 shows the population differences at 1-3 transition.

To further illustrate the dynamics of the population difference structure, the instantaneous values of the population inversion  $n$  after the third and fourth collisions for all three transitions are shown in Fig. 5; in Fig. 3 the same sections are denoted by  $a$  and  $b$ , respectively. From Fig. 2 we can see that at the 1-2 transition a grating formation takes place after pulse 2. However, this grating is not strictly harmonic. The polarization of the medium oscillates not only at the frequency of the 1-2 transition, but also at the frequencies of other transitions due to the presence of the third level. Figure 1 shows these oscillations. The amplitude of the grating is thus modulated in space.

We can also see from Fig. 2 that the third and subsequent pulses change the grating parameters, shifting in space, erasing or reducing the depth of modulation, etc. This distinguishes our case from that considered in rubidium in Ref. [69]. In those calculations, the shape of the resulting grating was closer to the harmonic, as in the two-level medium.

However, at the 1-3 transition (see Fig. 4), structures appear that are closer in form to harmonic structures. A more interesting situation occurs at the 2-3 transition (see Fig. 3). In this case, a microcavitylike structure with lateral Bragg mirrors is formed near the point  $z = 6.5\lambda_0$ . Near this point,

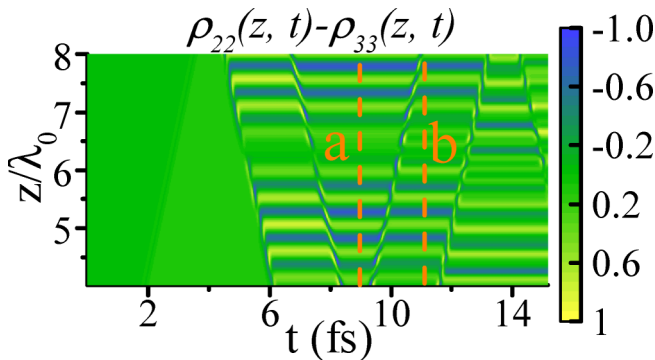


FIG. 3. Spatial and temporal dynamics of the medium population difference  $\rho_{22} - \rho_{33}$ .

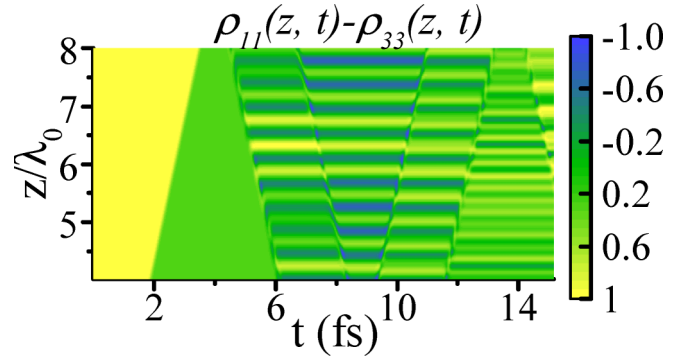


FIG. 4. Spatial and temporal dynamics of the medium population difference  $\rho_{11} - \rho_{33}$ .

the population difference has almost a constant value [see Fig. 5(a)]. A periodic grating of populations, the Bragg grating, appears on the sides. Similar microcavities appeared when unipolar rectangular pulses collided in a two-level medium [80]. After the passage of the next (fourth) pulse, the structure acquires a more complex character, namely, similar to the superposition of two periodic structures (“beats”), as shown in Fig. 5(b). It is interesting to note that after the third pulse, near the points  $z = 5\lambda_0$  and  $7.5\lambda_0$  the population difference for the 1-2 transition also stays at an almost constant value  $\rho_{22} - \rho_{33} \sim 0$  [see Fig. 5(a)]. Further evolution of the structure, as shown in Fig. 5(b), shows a complex beat form with multiple peaks.

Thus, as sometimes assumed, the effect of population gratings predicted in a two-level medium does not disappear when

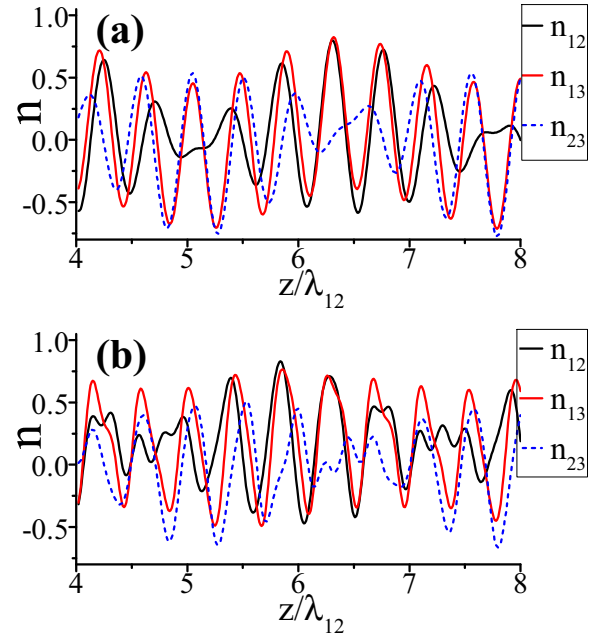


FIG. 5. Instantaneous value of the population differences  $n_{12}$  (black solid line),  $n_{13}$  [red (gray) solid line], and  $n_{23}$  [blue (gray) dashed line] as a function of the coordinate at a fixed moment in time at (a)  $t = 9.011$  fs and (b)  $t = 11.297$  fs corresponding to time sections  $a$  and  $b$  in Fig. 3.

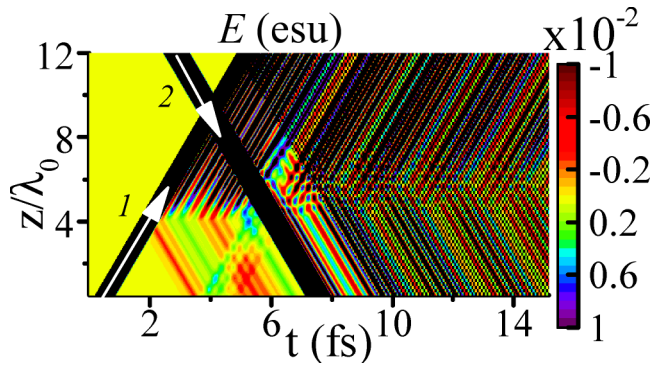


FIG. 6. Electric-field spatiotemporal distribution. The medium is excited by the two pulses 1 and 2 (thick black cross indicated by white arrows). The population relaxation time  $T_{1k} = T_1 = 100$  fs and the nondiagonal density-matrix-element (polarization) relaxation time  $T_{2k} = T_2 = 10$  fs. The other parameters are given in Table I. The medium is placed between the points  $z_1 = 4\lambda_0$  and  $8\lambda_0$ . The pulses overlap at the point  $z = 10\lambda_0$ , outside the medium.

additional levels of the medium are taken into account. The inclusion of the additional levels leads to a change in the form of the gratings, which may be different from the harmonic form. However, the harmonic form is possible as well [69]. Thus, the consideration of other levels of the medium results in a more varied dynamics of the system.

The difference between the shape of medium inversion gratings and harmonic gratings is easily explained by medium polarization behavior. While in a two-level medium, where there is only one resonant transition, the passing pulse 1 leaves behind a running wave of polarization oscillating at the transition frequency, in a multilevel medium the situation is more complicated. The passing pulse leaves behind oscillations of the coherence of the medium (nondiagonal elements of the density matrix) at each resonant transition of the medium. The resulting polarization will also oscillate at all transition frequencies of the medium. The polarization wave that is induced by the first pulse does not oscillate at a single frequency, as can be seen in Fig. 1. The second and subsequent pulses coherently control these oscillations, resulting in the appearance of nonharmonic grids at each medium resonant transition and forming more complex standing polarization structures.

#### IV. SUPERRADIANCE OF POLARIZATION WAVES AND INVERSION GRATINGS

The considered polarization waves exist for the coherence time of the medium  $T_2$ . These polarization structures and population gratings can emit electromagnetic radiation after the passage of excitation pulses [81]. This radiation can be considered as a superradiance of the medium [82,83], i.e., a collective spontaneous emission of the atoms of the medium that occurs in the absence of external excitation pulses.

The spatiotemporal behavior of the electric field in the integration domain obtained using the parameters from Table I is shown in Fig. 6. Corresponding polarization behavior is shown in Fig. 7. Only the values of the relaxation times

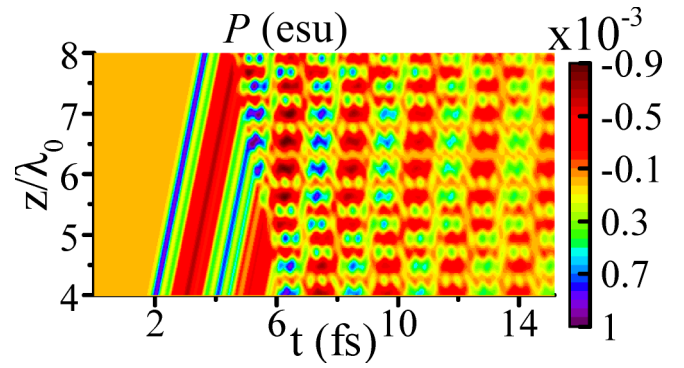


FIG. 7. Spatial and temporal dynamics of medium polarization  $P(z, t)$  for the case of Fig. 6.

have been changed as  $T_{1k} = T_1 = 100$  fs and  $T_{2k} = T_2 = 10$  fs to make the effect clearer. Only two pulses 1 and 2 have excited the medium in this example. After the pulses had passed through, the polarization waves were formed. They decay with time after the pulse passage can be seen in Fig. 7, while radiating light in both directions is shown in Fig. 6. Such radiation from the grating and the polarization of the medium should be taken into account in mode-locked lasers generating few-cycle pulses. In particular, in the case of ultrashort-cavity lasers, the mode-locked regime is due to coherent effects [84], so the radiation from such gratings and polarization structures can strongly affect the mode-locking regime.

#### V. CONCLUSION

In this work we have demonstrated the possibility of generating ultrafast control of population difference gratings in a three-level medium by a sequence of half-cycle attosecond pulses, based on the numerical solution of the system of Maxwell-Bloch equations. The parameters of the medium were taken to be close to those of an atomic hydrogen. The pulses did not overlap with each other in the medium. It was shown that considering additional levels of the medium also leads to the formation of gratings. However, the dynamics of the system may differ from the case of a two-level medium. This extends the applicability of previous results using two-level and other approximations.

It was shown that the shape of the gratings in general can differ from the purely harmonic one previously observed in the two-level medium. Also, the shapes of these gratings generated at different resonant transitions of the medium are very different from each other. The shape is almost harmonic at some transitions. At others, it is possible to form dynamic microcavities. This has previously been demonstrated in a two-level medium.

We have also considered the contribution of the superradiance effects, i.e., the collective emission of the atoms (in the absence of external excitation) produced by polarization waves and population gratings. After the pulses have passed, these polarization waves exist for the medium coherence time  $T_2$  and emit light in both the forward and backward directions of the medium. The emission of these gratings is important in mode-locked lasers operating in the few-cycle regime, as it

can strongly influence the dynamics of the generated pulses [84].

This study presents an avenue for further research in the optics of unipolar half-cycle pulses [8] and for the study of media with rapidly changing parameters, i.e., space-time photonic crystals [63–67].

## ACKNOWLEDGMENTS

The authors are grateful for support from Russian Science Foundation, through Project No. 23-12-00012 (Grating formation in multi-level medium), and State assignment of the Ioffe Institute, Topic No. 0040-2019-0017 (Superradiance by the polarization waves).

- 
- [1] F. Krausz and M. Ivanov, *Rev. Mod. Phys.* **81**, 163 (2009).
- [2] M. T. Hassan, T. T. Luu, A. Moulet, O. Raskazovskaya, P. Zhokhov, M. Garg, N. Karpowicz, A. M. Zheltikov, V. Pervak, F. Krausz, and E. Goulielmakis, *Nature (London)* **530**, 66 (2016).
- [3] F. Calegari, G. Sansone, S. Stagira, C. Vozzi, and M. Nisoli, *J. Phys. B* **49**, 062001 (2016).
- [4] K. Midorikawa, *Nat. Photonics* **16**, 267 (2022).
- [5] D. Hui, H. Alqattan, S. Yamada, V. Pervak, K. Yabana, and M. T. Hassan, *Nat. Photonics* **16**, 33 (2022).
- [6] H. Y. Kim, M. Garg, S. Mandal, L. Seiffert, T. Fennel, and E. Goulielmakis, *Nature (London)* **613**, 662 (2023).
- [7] <https://www.nobelprize.org/prizes/physics/2023/press-release/>.
- [8] R. M. Arkhipov, M. V. Arkhipov, and N. N. Rosanov, *Quantum Electron.* **50**, 801 (2020).
- [9] N. N. Rosanov, *Phys. Usp.* **66**, 1059 (2023).
- [10] J. D. Jackson, *Classical Electrodynamics* (Wiley, New York, 1962).
- [11] E. Bessonov, *Zh. Eksp. Teor. Fiz.* **80**, 852 (1981) [*Sov. Phys. JETP* **53**, 433 (1981)].
- [12] N. Rosanov, *Opt. Spectrosc.* **107**, 721 (2009).
- [13] R. Arkhipov, M. Arkhipov, P. Belov, Y. A. Tolmachev, and I. Babushkin, *Laser Phys. Lett.* **13**, 046001 (2016).
- [14] J. Xu, B. Shen, X. Zhang, Y. Shi, L. Ji, L. Zhang, T. Xu, W. Wang, X. Zhao, and Z. Xu, *Sci. Rep.* **8**, 2669 (2018).
- [15] A. V. Bogatskaya, E. A. Volkova, and A. M. Popov, *Phys. Rev. E* **104**, 025202 (2021).
- [16] A. Bogatskaya, E. Volkova, and A. Popov, *Plasma Sources Sci. Technol.* **30**, 085001 (2021).
- [17] S. Sazonov, *Laser Phys. Lett.* **18**, 105401 (2021).
- [18] R. Pang, Y. Wang, X. Yan, and B. Eliasson, *Phys. Rev. Appl.* **18**, 024024 (2022).
- [19] S. Wei, Y. Wang, X. Yan, and B. Eliasson, *Phys. Rev. E* **106**, 025203 (2022).
- [20] Q. Xin, Y. Wang, X. Yan, and B. Eliasson, *Phys. Rev. E* **107**, 035201 (2023).
- [21] M. I. Bakunov, A. V. Maslov, and M. V. Tsarev, *Phys. Rev. A* **95**, 063817 (2017).
- [22] M. V. Tsarev and M. I. Bakunov, *Opt. Express* **27**, 5154 (2019).
- [23] A. Plachenov and N. Rosanov, *Radiophys. Quantum Electron.* **65**, 1003 (2022).
- [24] A. Pakhomov, M. Arkhipov, N. Rosanov, and R. Arkhipov, *Phys. Rev. A* **106**, 053506 (2022).
- [25] M. Arkhipov, A. Pakhomov, R. Arkhipov, and N. Rosanov, *Opt. Lett.* **48**, 4637 (2023).
- [26] V. V. Kozlov, N. N. Rosanov, C. De Angelis, and S. Wabnitz, *Phys. Rev. A* **84**, 023818 (2011).
- [27] G. Naumenko, M. Shevelev, and K. Popov, *Phys. Part. Nuclei Lett.* **17**, 834 (2020).
- [28] M. V. Arkhipov, A. N. Tsyarkin, A. M. Zhukova, A. O. Ismagilov, A. V. Pakhomov, N. N. Rosanov, and R. M. Arkhipov, *JETP Lett.* **115**, 1 (2022).
- [29] C. Raman, C. W. S. Conover, C. I. Sukenik, and P. H. Bucksbaum, *Phys. Rev. Lett.* **76**, 2436 (1996).
- [30] P. L. Shkolnikov, A. E. Kaplan, and S. F. Straub, *Phys. Rev. A* **59**, 490 (1999).
- [31] R. Arkhipov, A. Pakhomov, M. Arkhipov, A. Demircan, U. Morgner, N. Rosanov, and I. Babushkin, *Opt. Express* **28**, 17020 (2020).
- [32] P. H. Bucksbaum, *AIP Conf. Proc.* **323**, 416 (1994).
- [33] D. Dimitrovski, E. A. Solov'ev, and J. S. Briggs, *Phys. Rev. A* **72**, 043411 (2005).
- [34] N. Rosanov, D. Tumakov, M. Arkhipov, and R. Arkhipov, *Phys. Rev. A* **104**, 063101 (2021).
- [35] A. Pakhomov, M. Arkhipov, N. Rosanov, and R. Arkhipov, *Phys. Rev. A* **105**, 043103 (2022).
- [36] R. Arkhipov, P. Belov, A. Pakhomov, M. Arkhipov, and N. Rosanov, *J. Opt. Soc. Am. B* **41**, 285 (2024).
- [37] R. M. Arkhipov, M. V. Arkhipov, and N. N. Rosanov, *JETP Lett.* **111**, 484 (2020).
- [38] H. J. Eichler, P. Günter, and D. W. Pohl, *Laser-Induced Dynamic Gratings* (Springer, Berlin, 1981).
- [39] S. Vasiliev, O. Medvedkov, I. Korolev, A. Bozhkov, A. Kurkov, and E. Dianov, *Quantum Electron.* **35**, 1085 (2005).
- [40] R. Kashyap, *Fiber Bragg Gratings* (Academic, New York, 2009).
- [41] I. D. Abella, N. A. Kurnit, and S. R. Hartmann, *Phys. Rev.* **141**, 391 (1966).
- [42] E. I. Shtyrkov, V. S. Lobkov, and N. G. Yarmukhametov, *JETP Lett.* **27**, 648 (1978).
- [43] S. A. Moiseev and E. I. Shtyrkov, *Sov. J. Quantum Electron.* **21**, 403 (1991).
- [44] R. M. Arkhipov, M. V. Arkhipov, I. Babushkin, A. Demircan, U. Morgner, and N. N. Rosanov, *Opt. Lett.* **41**, 4983 (2016).
- [45] R. M. Arkhipov, A. V. Pakhomov, M. V. Arkhipov, I. V. Babushkin, A. Demircan, U. Morgner, and N. N. Rosanov, *Sci. Rep.* **7**, 12467 (2017).
- [46] R. M. Arkhipov, A. V. Pakhomov, M. V. Arkhipov, I. V. Babushkin, A. Demircan, U. Morgner, and N. N. Rosanov, *Sci. Rep.* **11**, 1961 (2021).
- [47] H. Zhang, S. Zhang, S. Li, and X. Ma, *Opt. Commun.* **462**, 125182 (2020).
- [48] S. Zhang, S. Li, Y. Bai, and K. Huang, *J. Nanophotonics* **17**, 016013 (2023).
- [49] E. Shtyrkov and V. Samartsev, *Phys. Status Solidi A* **45**, 647 (1978).
- [50] E. I. Shtyrkov, *Opt. Spectrosc.* **114**, 96 (2013).

- [51] R. Arkhipov, M. Arkhipov, A. Pakhomov, and N. Rosanov, *Laser Phys.* **32**, 066002 (2022).
- [52] R. Arkhipov, *JETP Lett.* **113**, 611 (2021).
- [53] X. Song, W. Yang, Z. Zeng, R. Li, and Z. Xu, *Phys. Rev. A* **82**, 053821 (2010).
- [54] S. Hughes, *Phys. Rev. Lett.* **81**, 3363 (1998).
- [55] A. V. Tarasishin, S. A. Magnitskii, V. Shuvaev, and A. Zheltikov, *Opt. Express* **8**, 452 (2001).
- [56] D. V. Novitsky, *Phys. Rev. A* **84**, 013817 (2011).
- [57] D. V. Novitsky, *Phys. Rev. A* **85**, 043813 (2012).
- [58] D. V. Novitsky, *Phys. Rev. A* **86**, 063835 (2012).
- [59] D. V. Novitsky, *J. Phys. B* **47**, 095401 (2014).
- [60] S. Sazonov and A. Sobolevskii, *J. Exp. Theor. Phys.* **96**, 807 (2003).
- [61] F. Biancalana, A. Amann, A. V. Uskov, and E. P. O'Reilly, *Phys. Rev. E* **75**, 046607 (2007).
- [62] J. R. Zurita-Sánchez, P. Halevi, and J. C. Cervantes-González, *Phys. Rev. A* **79**, 053821 (2009).
- [63] E. Lustig, Y. Sharabi, and M. Segev, *Optica* **5**, 1390 (2018).
- [64] Y. Sharabi, A. Dikopoltsev, E. Lustig, Y. Lumer, and M. Segev, *Optica* **9**, 585 (2022).
- [65] M. Lyubarov, Y. Lumer, A. Dikopoltsev, E. Lustig, Y. Sharabi, and M. Segev, *Science* **377**, 425 (2022).
- [66] E. Lustig, O. Segal, S. Saha, E. Bordo, S. N. Chowdhury, Y. Sharabi, A. Fleischer, A. Boltasseva, O. Cohen, V. M. Shalaev, and M. Segev, *Nanophotonics* **12**, 2221 (2023).
- [67] A. Boltasseva, V. M. Shalaev, and M. Segev, *Opt. Mater. Express* **14**, 592 (2024).
- [68] K. Xu, M. Fang, J. Fen, C. Wang, G. Xie, and Z. Huang, *Opt. Lett.* **49**, 842 (2024).
- [69] R. Arkhipov, *Laser Phys.* **34**, 065301 (2024).
- [70] L. Allen and J. H. Eberly, *Optical Resonance and Two-Level Atoms* (Wiley, New York, 1975).
- [71] A. Yariv, *Quantum Electronics* (Wiley, New York, 1989).
- [72] E. Frish, *Optical Spectra of Atoms* (Fizmatgiz, Moscow, 1963).
- [73] W. Wiese and J. Fuhr, *J. Phys. Chem. Ref. Data* **38**, 565 (2009).
- [74] N. N. Rosanov, *Opt. Spectrosc.* **127**, 1050 (2019).
- [75] A. Pusch, J. M. Hamm, and O. Hess, *Phys. Rev. A* **82**, 023805 (2010).
- [76] P. Belov and R. Arkhipov, *Micro Nanostruct.* **180**, 207607 (2023).
- [77] A. de las Heras, C. Hernández-García, J. Serrano, A. Prodanov, D. Popmintchev, T. Popmintchev, and L. Plaja, [arXiv:2404.04053](https://arxiv.org/abs/2404.04053).
- [78] M. F. Ciappina, J. A. Pérez-Hernández, A. S. Landsman, T. Zimmermann, M. Lewenstein, L. Roso, and F. Krausz, *Phys. Rev. Lett.* **114**, 143902 (2015).
- [79] O. D. Mücke, T. Tritschler, M. Wegener, U. Morgner, and F. X. Kärtner, *Phys. Rev. Lett.* **87**, 057401 (2001).
- [80] O. Diachkova, R. Arkhipov, M. Arkhipov, A. Pakhomov, and N. Rosanov, *Opt. Commun.* **538**, 129475 (2023).
- [81] V. V. Zheleznyakov, V. V. Kocharovskiy, and V. V. Kocharovskiy, *Sov. Phys. Usp.* **32**, 835 (1989).
- [82] K. Cong, Q. Zhang, Y. Wang, G. T. Noe, A. Belyanin, and J. Kono, *J. Opt. Soc. Am. B* **33**, C80 (2016).
- [83] V. V. Kocharovskiy, V. V. Zheleznyakov, E. R. Kocharovskaya, and V. V. Kocharovskiy, *Phys. Usp.* **60**, 345 (2017).
- [84] R. Arkhipov, M. Arkhipov, A. Pakhomov, I. Babushkin, and N. Rosanov, *Phys. Rev. A* **105**, 013526 (2022).